Inorg. Chem. **2008**, *47*, 4779−4784

Determination of the Spin−Lattice Relevant for the Quaternary Magnetic Oxide $Bi_4Cu_3V_2O_{14}$ on the Basis of Tight-Binding and Density Functional Calculations

Hyun-Joo Koo* and Myung-Hwan Whangbo*

Department of Chemistry and Research Institute of Basic Science, Kyung Hee University, Seoul 130-701, Korea, and Department of Chemistry, North Carolina State University, Raleigh, North Carolina 27695-8204

Received February 1, 2008

The quaternary magnetic oxide $Bi_4Cu_3V_2O_{14}$ consists of Cu_4O_8 triple chains made up of corner-sharing CuO_4 square planes. To determine its spin−lattice, the spin exchange interactions of $Bi_4Cu_3V_2O_{14}$ were evaluated by performing a spin dimer analysis based on tight-binding calculations and a mapping analysis based on first principles density functional theory calculations. Both calculations show that the spin−lattice of $Bi_4Cu_3V_2O_{14}$ is not an antiferromagnetically coupled diamond chain, which results from an idealized view of the structure of the Cu_4O_8 triple chain and a neglect of super-superexchange interactions. The correct spin−lattice is an antiferromagnetic chain made up of antiferromagnetic linear trimers coupled through their midpoints via super-superexchange interaction, which predicts that $Bi_4Cu_3V_2O_{14}$ has an antiferromagnetic spin ground state and has no spin frustration, both in agreement with experiment.

1. Introduction

In recent years, geometric spin frustration in low-dimensional quantum spin systems has received much attention.[1] The archetypal example of a one-dimensional (1D) spin−lattice of Cu^{2+} ions with geometric spin frustration is the CuO_2 ribbon chain made up of edge-sharing CuO_4 square planes. In such CuO_2 chains present in the multiferroic compounds $LiCuVO_4$[2] and $LiCu_2O_2$,[3] the geometric spin frustration in the CuO_2 ribbon chains makes the spins undergo a spiral spin ordering, which in turn induces ferroelectricity because this spin ordering removes inversion symmetry.[4] Other 1D spin−lattices with spin frustration include the δ chain model used for $[Cu(bpy)H_2O]$-$[Cu(bpy)(mal)H_2O](ClO_4)_2$ (H_2mal = malonic acid, bpy = 2,2′-bipyridine)[5] and the diamond chain model used for $Cu_3(CO_3)_2(OH)_2$.[6]

The diamond chain model has also been employed to describe the magnetic properties of the quaternary magnetic oxide $Bi_4Cu_3V_2O_{14}$,[7−10] but there are puzzling observations not explained by this model. The structure of the quaternary magnetic oxide $Bi_4Cu_3V_2O_{14}$[7] can be described in terms of $Cu_3V_2O_{12}$ chains separated by Bi_4O_2 chains running along the a direction (Figure 1a). In each $Cu_3V_2O_{12}$ chain (Figure 2a), corner-sharing CuO_4 square planes form a Cu_3O_8 triple chain consisting of three nearly coplanar CuO_4 chains, and

* To whom correspondence should be addressed. E-mail: hjkoo@khu.ac.kr (H.-J.K); mike_whangbo@ncsu.edu (M.-H.W.).

(1) (a) Greedan, J. E. *J. Mater. Chem.* **2001**, *11*, 37. and references cited therein. (b) Dai, D.; Whangbo, M.-H. *J. Chem. Phys.* **2004**, *121*, 672.
(2) (a) Gibson, B. J.; Kremer, R. K.; Prokofiev, A. V.; Assmus, W.; McIntyre, G. J. *Physica B (Amsterdam, Neth.)* **2004**, *350*, e253. (b) Naito, Y.; Sato, K.; Yasui, Y.; Kobayashi, Y.; Kobayashi, Y.; Sato, M. *J. Phys. Soc. Jpn.* **2007**, *76*, 023708.
(3) (a) Masuda, T.; Zheludev, A.; Bush, A.; Markina, M.; Vasiliev, A. *Phys. Rev. Lett.* **2004**, *92*, 177201. (b) Park, S.; Choi, Y. J.; Zhang, C. L.; Cheong, S.-W. *Phys. Rev. Lett.* **2007**, *98*, 057601.
(4) Xiang, H. J.; Whangbo, M.-H. *Phys. Rev. Lett.* **2007**, *99*, 257203.
(5) Kunimoto, T.; Kamikawa, T.; Inagaki, Y.; Okubo, S.; Ohta, H.; Kikuchi, H.; Saito, T.; Azuma, M.; Takano, M. *Physica B (Amsterdam, Neth.)* **2003**, *329−333*, 1057.
(6) (a) Kikuchi, H.; Fujii, Y.; Chiba, M.; Mitsudo, S.; Idehara, T. *Physica B (Amsterdam, Neth.)* **2003**, *329−333*, 967. (b) Kamikawa, T.; Okubo, S.; Kunimoto, T.; Ohta, H.; Inagaki, Y.; Kikuchi, H.; Saito, T.; Azuma, M.; Takano, M. *Physica B (Amsterdam, Neth.)* **2003**, *329−333*, 988.
(7) Deacon, G. B.; Gatehouse, B. M.; Ward, G. N. *Acta Crystallogr., Sect. C* **1994**, *50*, 1178.
(8) Sakurai, H.; Yoshimura, K.; Kosuge, K.; Tsujii, N.; Abe, H.; Kitazawa, H.; Kido, G.; Michor, H.; Hilscher, G. *J. Phys. Soc. Jpn.* **2002**, *71*, 1161.
(9) Okubo, S.; Hirano, T.; Inagaki, Y.; Ohta, H.; Sakurai, H.; Yoshimura, H.; Kosuge, K. *Physica B (Amsterdam, Neth.)* **2004**, *346*, 65.
(10) Okamoto, K.; Tonegawa, T.; Kaburagi, M. *J. Phys.: Condens. Matter* **2003**, *15*, 5979.

10.1021/ic800216j CCC: $40.75
Published on Web 05/03/2008

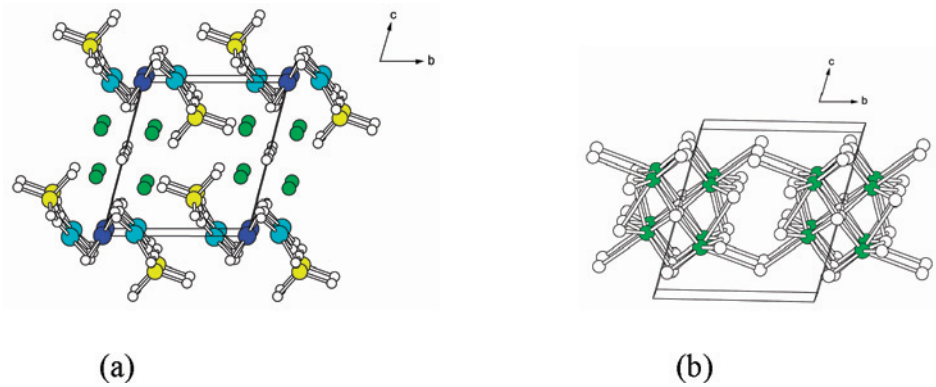

Figure 1. (a) Perspective view of the crystal structure of $Bi_4Cu_3V_2O_{14}$, where the green, cyan, blue, yellow, and white circles represent Bi, Cu1, Cu2, V, and O atoms, respectively. For simplicity, the Bi−O bonds and the long Cu−O bonds are not shown. (b) Perspective view of the coordinate environments of the Bi atoms in $Bi_4Cu_3V_2O_{14}$.

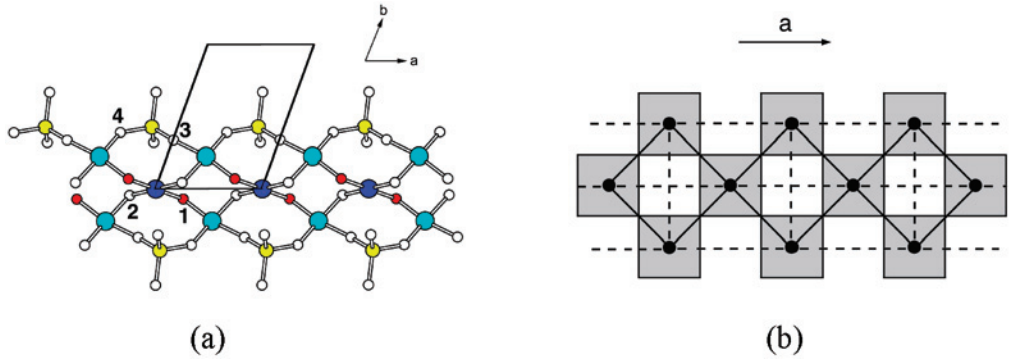

Figure 2. (a) Perspective view of the $Cu_3V_2O_{12}$ chain along the a direction in $Bi_4Cu_3V_2O_{14}$. The numbers 1, 2, 3, and 4 refer to the O1, O2, O3, and O4 atoms, respectively. The Cu1, Cu2, and V atoms are represented by cyan, blue, and yellow circles, respectively, while the O1 and O2 atoms of the $Cu2O_4$ square planes are distinguished by red and white circles, respectively. (b) Idealized arrangement of the CuO_4 square planes in the $Cu_3V_2O_{12}$ chain in which all of the CuO_4 units have the shape of an ideal square plane so that all of the SE exchange paths (solid lines) are identical, as are all of the SSE exchange paths (dashed lines).

the outer two CuO_4 chains are capped by VO_4 tetrahedra via corner-sharing. In each Bi_4O_2 chain, every O atom is located at the center of a Bi_4 tetrahedron, and each Bi_4O_2 chain is surrounded by four $Cu_3V_2O_{12}$ chains such that every Bi atom is surrounded by eight O atoms (Figure 1b). With the oxidation assignment $(Bi^{3+})_4(Cu^{2+})_3(V^{5+})_2(O^{2-})_{14}$ for $Bi_4Cu_3V_2O_{14}$, only the Cu^{2+} ions have unpaired spins and are responsible for the magnetic properties of $Bi_4Cu_3V_2O_{14}$. Therefore, if the CuO_4 units of the Cu_3O_8 triple chain are regarded as ideal square planes, the Cu^{2+} ions form a diamond chain with identical Cu−O−Cu superexchange (SE) interactions and identical Cu−O···O−Cu super-superexchange (SSE) interactions across the diagonal directions of each diamond (Figure 2b). The magnetic susceptibility of $Bi_4Cu_3V_2O_{14}$ shows a characteristic feature of a low-dimensional antiferromagnet (i.e., a broad maximum around 20.5 K), and the susceptibility between 100 and 320 K is well-reproduced by the Curie−Weiss law with $\theta = -48.1$ K.[8] The specific heat measurement shows a λ-type peak at $T_N = 6$ K, and the ^{51}V NMR measurements at 4.2 K indicate an antiferromagnetic (AFM) spin ground state. If we neglect the SSE interactions and assume that the SE interactions are identical, the spin−lattice of the Cu_3O_8 triple chain becomes a diamond chain, and the ground state of such a chain is ferrimagnetic if the SE interactions are AFM. However, $Bi_4Cu_3V_2O_{14}$ does not exhibit a ferrimagnetic behavior in the magnetic susceptibility above T_N and in the magnetization curve below T_N.[8] Therefore, the SSE interactions between Cu^{2+} ions cannot be ignored. The high-field ESR study[9] showed that the diamond chain model with AFM superexchange is inadequate for describing the magnetic properties of $Bi_4Cu_3V_2O_{14}$. It has been suggested[10] that $Bi_4Cu_3V_2O_{14}$ is in a spin fluid state above T_N, since a ferrimagnetic behavior is not seen in the susceptibility above T_N.

The magnetic properties of $Bi_4Cu_3V_2O_{14}$ present puzzling features, as mentioned above, primarily because the structure of the Cu_3O_8 triple chain is not as symmetrical as idealized in Figure 2b and because SSE interactions can be stronger than SE interactions.[11,12] At present, the precise nature of its spin−lattice is unknown, and hence it is not certain whether the diamond chain model is relevant even to a first approximation. To remedy this undesirable situation, it is necessary to evaluate the spin exchange interactions of $Bi_4Cu_3V_2O_{14}$ by appropriate electronic structure calculations. In the present work, we evaluate these interactions by performing a spin dimer analysis[11,12] based on extended Hückel tight

(11) For reviews see:(a) Whangbo, M.-H.; Koo, H.-J.; Dai, D. *J. Solid State Chem.* **2003**, *176*, 417. (b) Whangbo, M.-H.; Dai, D.; Koo, H.-J. *Solid State Sci.* **2005**, *7*, 827.

(12) (a) Koo, H.-J.; Whangbo, M.-H. *Inorg. Chem.* **2001**, *40*, 2169. (b) Koo, H.-J.; Whangbo, M.-H.; VerNooy, P. D.; Torardi, C. C.; Marshall, W. J. *Inorg. Chem.* **2002**, *41*, 4664. (c) Whangbo, M.-H.; Koo, H.-J.; Dai, D.; Jung, D. *Inorg. Chem.* **2003**, *42*, 3898. (d) Koo, H.-J.; Whangbo, M.-H.; Lee, K.-S. *Inorg. Chem.* **2003**, *42*, 5932. (e) Dai, D.; Koo, H.-J.; Whangbo, M.-H. *Inorg. Chem.* **2004**, *43*, 4026. (f) Koo, H.-J.; Dai, D.; Whangbo, M.-H. *Inorg. Chem.* **2005**, *44*, 4359.

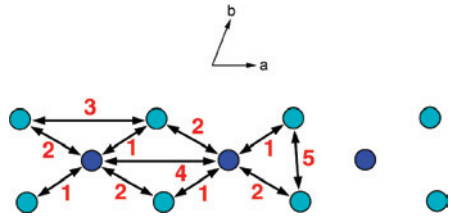

Figure 3. Schematic representations of the spin exchange paths in the $Cu_3V_2O_{12}$ chain, where the numbers 1−5 refer to the spin exchange paths J_1−J_5, respectively.

Table 1. Geometrical Parameters Associated with the Spin Exchange Paths of $Bi_4Cu_3V_2O_{14}$[a]

nature	path	Cu···Cu	Cu−O	∠Cu−O−Cu
SE	J_1	3.064	1.916, 1.988	103.4
	J_2	3.289	1.970, 1.941	114.5
SSE	J_3	5.317	2.729	159.2, 109.7
		2.687	142.6, 124.0	
	J_4	5.317	2.646	133.4, 130.8
		2.646	133.4, 130.8	
	J_5	3.484	2.906	78.4, 80.1
			2.906	78.4, 80.1

[a] The bond distances are in units of Ångstrom, and the bond angles are in units of degrees.

Table 2. Relative Values of $(\Delta e)^2$ [in $(meV)^2$] of SE and SSE Paths in $Bi_4Cu_3V_2O_{14}$

	$x = 0.00$	$x = 0.05$	$x = 0.10$
J_1	0.15	0.16	0.14
J_2	1.00	0.73	0.52
J_3	0.42 (0.16)[a]	0.44 (0.19)[a]	0.43 (0.20)[a]
J_4	0.96	1.00	1.00
J_5	0.03	0.02	0.01

[a] The numbers in parentheses are obtained with VO_4 bridges attached.

binding (EHTB) calculations[13] as well as a mapping analysis[11a,14–16] based on first principles density functional theory (DFT) electronic band structure calculations.

2. Structure and Spin Dimer Analyses

$Bi_4Cu_3V_2O_{14}$ has two nonequivalent Cu atoms, Cu1 and Cu2 (Figure 2a). Both Cu atoms form CuO_4 square planes with Cu1−O = 1.941, 1.916, 1.943, and 1.927 Å and Cu2−O = 1.970 (×2) and 1.988 (×2) Å, if the long apical Cu−O bonds (i.e., Cu1−O = 2.751 Å and Cu2−O = 2.574 Å) are neglected. Each $Cu2O_4$ square plane is corner-shared with four neighboring $Cu1O_4$ square planes, while each $Cu1O_4$ is corner-shared with two neighboring $Cu2O_4$ square planes and two neighboring VO_4 tetrahedra (Figure 2a). Since the oxygen atoms O1, O2, O3, and O4 of the $Cu_3V_2O_{12}$ chain are not equivalent, the SE paths J_1 and J_2 should be nonequivalent, and so should be the SSE paths J_3, J_4, and J_5 (Figure 3). The geometrical parameters associated with the spin exchange paths J_1−J_5 are summarized in Table 1.

In a spin dimer analysis based on EHTB calculations, the strength of a spin exchange interaction between two spin sites is estimated by considering only the antiferromagnetic contribution J_{AF} to the spin exchange:[11,17]

$$J_{AF} \approx \frac{(\Delta e)^2}{U_{eff}} \quad (1)$$

where U_{eff} is the effective on-site repulsion that is essentially a constant for a given compound. In the present work, the $(\Delta e)^2$ values for various spin dimers are evaluated by performing EHTB calculations.[13] For a variety of magnetic solids of transition metal ions, it has been found that their magnetic properties are well-described by the $(\Delta e)^2$ values obtained from EHTB calculations, when both the d orbitals of the transition metal ions and the s/p orbitals of its surrounding ligands are represented by double-ζ Slater-type orbitals (DZ-STO).[18] The atomic parameters used in our calculations are summarized in the Table S1 of the Supporting Information. The radial part of a DZ-STO is expressed as

$$r^{n-1}[c_1 \exp(-\zeta_1 r) + c_2 \exp(-\zeta_2 r)]$$

where n is the principal quantum number and the exponents ζ_1 and ζ_2 describe contracted and diffuse STOs, respectively (i.e., $\zeta_1 > \zeta_2$). The diffuse STO provides an orbital tail that enhances overlap between O atoms in the O···O contacts of the Cu−O···O−Cu SSE paths. The $(\Delta e)^2$ values are affected most sensitively by the exponent ζ_2 of the diffuse O 2p orbital. The ζ_2 values taken from results of electronic structure calculations for neutral atoms[18] may not be diffuse enough to describe O^{2-} ions. To make the O 2p orbital more diffuse, the ζ_2 value should be reduced. To assess how the diffuseness of the O 2p orbital affects the relative strengths of the SSE interactions, we replace ζ_2 with $(1 - x)\zeta_2$ and calculate the $(\Delta e)^2$ values for three values of x, that is, 0.00, 0.05, and 0.10. Results of our spin dimer analysis are summarized in Table 2.

Table 2 shows that the two strongest spin exchange interactions are the SE interaction J_2 and the SSE interaction J_4. The SE interaction J_2 is much stronger than the SE interaction J_1. This is easily accounted for because

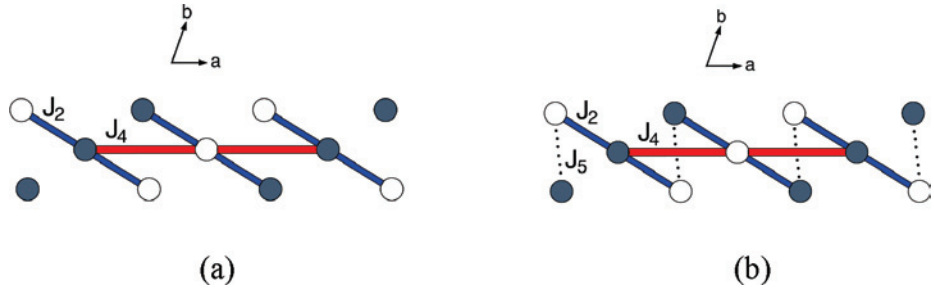

Figure 4. Spin−lattice of $Bi_4Cu_3V_2O_{14}$ suggested from (a) the spin dimer analysis based on EHTB calculations and (b) the mapping analysis based on GGA+U calculations. The gray and white circles represent the up and down spin states of Cu atoms, respectively.

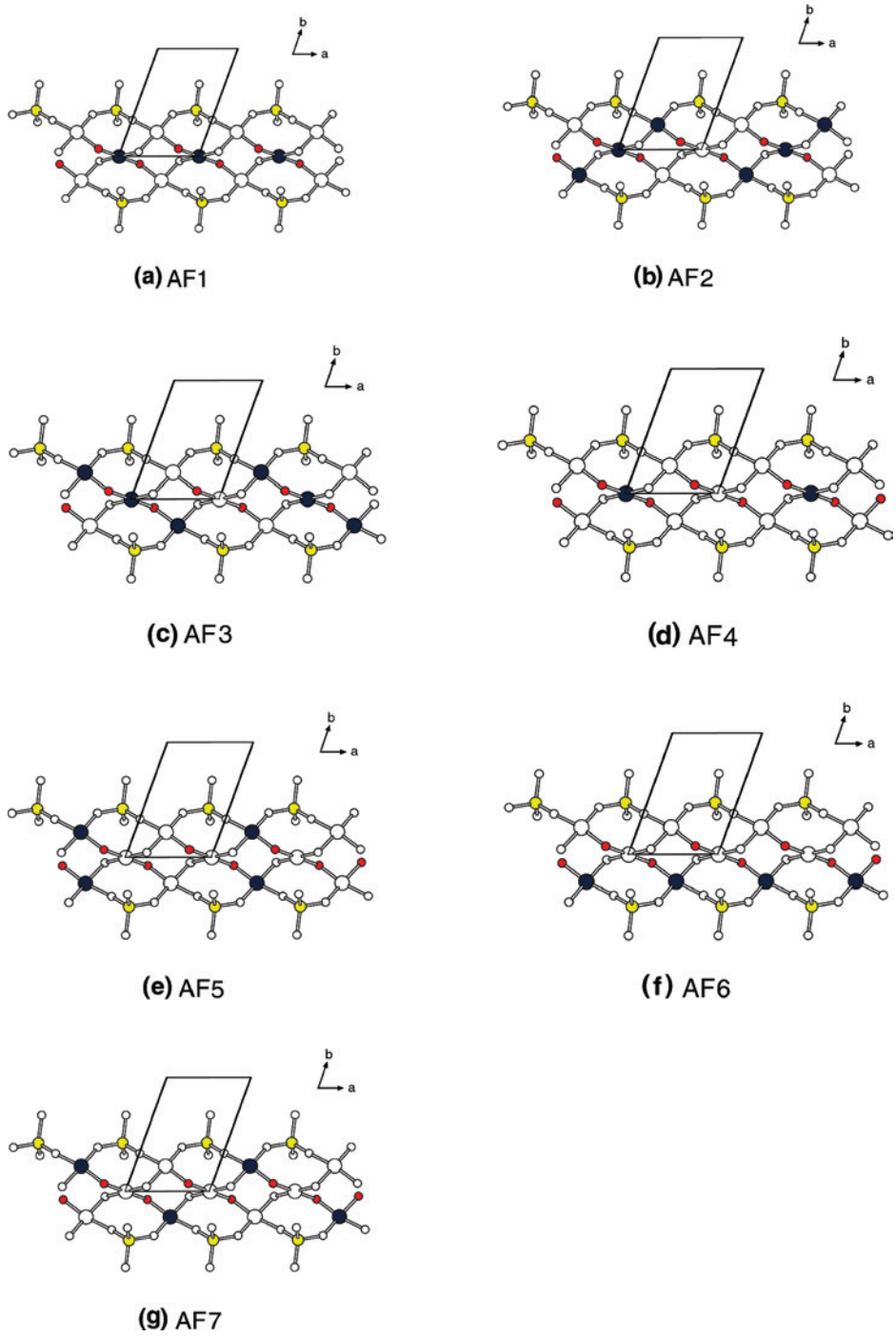

Figure 5. Ordered spin arrangements (a) AF1, (b) AF2, (c) AF3, (d) AF4, (e) AF5, (f) AF6, and (g) AF7. The large gray and white circles refer to the up and down spin Cu sites, respectively.

the ∠Cu−O−Cu angle associated with the SE interaction is considerably larger for J_2 than for J_1 (Table 1). J_4 is the strongest one of the three SSE interactions J_3, J_4, and J_5, which is explained by the fact that the two O···O contact distances associated with J_4 are symmetrical and are substantially shorter compared with the corresponding O···O distances associated with J_3 and J_5 (Table 1). The SE interaction J_2 forms isolated linear AFM trimers and is comparable in magnitude to the SSE interaction J_4. When the ζ_2 value of the O 2p orbital becomes more diffuse, the J_4 interaction eventually becomes stronger than the SE interaction J_2. The SSE path J_3 has the VO_4 bridging unit. To examine the effect of the VO_4 units on J_3, we calculated the $(\Delta e)^2$ values with and without the VO_4 units. As summarized in Table 2, the magnitude of the SSE interaction J_3 is strongly reduced when the VO_4 unit is included. This is due to the fact that the antibonding combination of the magnetic orbitals of the two Cu^{2+} ions is lowered in energy by the d_π orbital of the V^{5+} ion of the VO_4 bridge, as found for $LiCuVO_4$.[12e] As depicted in Figure 4a, the linear AFM trimers defined by the SE interaction J_2 are antiferromagnetically coupled by the SSE interactions J_4 through their middle Cu^{2+} ions to form an AFM chain along the a direction. In essence, the

spin−lattice of the $Cu_3V_2O_{12}$ chain is not a diamond chain but an AFM chain made up of linear AFM trimers. This picture does not depend on the variation of the diffuseness of the O 2p orbital, because the latter does not change the fact that J_2 and J_4 are the two strongest spin exchange interactions.

The above picture for the spin−lattice of $Bi_4Cu_3V_2O_{14}$ derived from the spin dimer analysis, that is, an AFM chain of linear AFM trimers, predicts an antiferromagnetically ordered spin ground state for $Bi_4Cu_3V_2O_{14}$, in agreement with experimental results. Nevertheless, the relative strengths of J_2 and J_4 depend on the diffuseness of the O 2p orbital, and the strength of J_3 depends on whether the VO_4 unit is included or not. To resolve these uncertainties and obtain more precise values for the spin exchange parameters, it is necessary to evaluate the spin exchange interactions of $Bi_4Cu_3V_2O_{14}$ on the basis of first principles DFT electronic structure calculations, as discussed in the next section.

3. Quantitative Evaluation of Spin Exchange Interaction Parameters

To determine the spin exchange parameters J_1-J_5 on the basis of first principles DFT electronic band structure calculations, we first calculate the total energies of several ordered spin states of $Bi_4Cu_3V_2O_{14}$ and then relate the energy differences between these states to the corresponding energy differences expected from the spin Hamiltonian:

$$\hat{H} = -\sum_{i<j} J_{ij}\hat{S}_i \cdot \hat{S}_j \tag{2}$$

where J_{ij} ($= J_1-J_5$) is the spin exchange parameter for the spin exchange interaction between the spin sites i and j, while $\hat{S}_i$ and $\hat{S}_j$ are the spin angular momentum operators at the spin sites i and j, respectively. Since there are five parameters to determine, at least six or more ordered spin states are necessary for this mapping analysis. We used the seven ordered spin arrangements shown in Figure 5. The total energies of these states were calculated by performing spin-polarized DFT electronic band structure calculations with the projected augmented-wave method encoded in the Vienna ab initio simulation package.[19] Our calculations employed the generalized gradient approximation (GGA) for the exchange and correlation correction,[20] the plane wave cutoff energy of 400 eV, the on-site repulsion U on copper, and the sampling of the irreducible Brillouin zone with 100 k points. To see how the value of U affects our results, we performed GGA plus onsite repulsion (GGA+U) calculations[21] with $U = 5$, 6, and 7 eV.

Our GGA+U calculations show that the AF2 state is the most stable state. The relative energies of the seven ordered spin states with respect to that of the AF2 state are listed in Table 3. To extract the values of the spin exchange parameters J_1-J_5 from the above electronic structure calculations, we express the total spin exchange interaction energies of the seven ordered spin states in terms of the spin Hamiltonian given in eq 2. By applying the energy expressions obtained for spin dimers with N unpaired spins per spin site (in the present case, $N = 1$),[22] the total spin exchange energies per formula units are written as

$$E_{AF1} = (2J_1 + 2J_2 - 2J_3 - J_4 - J_5)N^2/4 \tag{3}$$

$$E_{AF2} = (-2J_1 + 2J_2 + 2J_3 + J_4 + J_5)N^2/4 \tag{4}$$

$$E_{AF3} = (2J_1 - 2J_2 + 2J_3 + J_4 + J_5)N^2/4 \tag{5}$$

$$E_{AF4} = (-2J_3 + J_4 - J_5)N^2/4 \tag{6}$$

$$E_{AF5} = (2J_3 - J_4 - J_5)N^2/4 \tag{7}$$

$$E_{AF6} = (-2J_3 - J_4 + J_5)N^2/4 \tag{8}$$

$$E_{AF7} = (2J_3 - J_4 + J_5)N^2/4 \tag{9}$$

From the above equations, the spin exchange parameters J_1-J_5 can be expressed in terms of state energy differences as follows:

$$J_5 = \frac{1}{2}\left(\frac{4}{N^2}\right)(E_{AF7} - E_{AF5}) \tag{10}$$

$$J_3 = \frac{1}{4}\left(\frac{4}{N^2}\right)(E_{AF7} - E_{AF6}) \tag{11}$$

$$J_4 = \frac{1}{2}\left[\left(\frac{4}{N^2}\right)(E_{AF4} - E_{AF5}) + 4J_3\right] \tag{12}$$

$$J_2 = \frac{1}{4}\left[\left(\frac{4}{N^2}\right)(E_{AF1} - E_{AF3}) + 4J_3 + 2J_4 + 2J_5\right] \tag{13}$$

$$J_1 = \frac{1}{4}\left[\left(\frac{4}{N^2}\right)(E_{AF1} - E_{AF2}) + 4J_3 + 2J_4 + 2J_5\right] \tag{14}$$

The J_1-J_5 values calculated from the above expressions are summarized in Table 4. For all values of U employed, the two strongest spin exchange interactions are J_2 and J_4, which are both AFM. This result confirms the prediction of the spin dimer analysis based on EHTB calculations. Furthermore, J_4 is slightly stronger than J_2, which agrees with the result of the spin dimer analysis obtained from the use of a more diffuse O 2p orbital. The spin exchange interactions J_1 and J_5 are weakly antiferromagnetic, while the spin exchange

(13) (a) Hoffmann, R. *J. Chem. Phys.* **1963**, *39*, 1397. (b) Our calculations were carried out by employing the SAMOA (Structure and Molecular Orbital Analyzer) program package. This program can be downloaded free of charge from the Web site. http://chvamw.chem.ncsu.edu/ (accessed Apr 2008).

(14) Noodleman, L. *J. Chem. Phys.* **1981**, *74*, 5737.

(15) Illas, F.; Moreira, I. d. P. R.; de Graaf, C.; Barone, V. *Theor. Chem. Acc.* **2000**, *104*, 265. and references cited therein.

(16) (a) Chartier, A.; D'Arco, P.; Dovesi, R.; Saunders, V. R. *Phys. Rev. B: Condens. Matter Mater. Phys.* **1999**, *60*, 14042. and references cited therein. (b) Dai, D.; Whangbo, M.-H.; Koo, H.-J.; Rocquefelte, X.; Jobic, S.; Villesuzanne, A. *Inorg. Chem.* **2005**, *44*, 2407.

(17) Hay, P. J.; Thibeault, J. C.; Hoffmann, R. *J. Am. Chem. Soc.* **1975**, *97*, 4884.

(18) Clementi, E.; Roetti, C. *At. Data Nucl. Data Tables* **1974**, *14*, 177.

(19) (a) Kresse, G.; Hafner, J. *Phys. Rev. B: Condens. Matter Mater. Phys.* **1993**, *62*, 558. (b) Kresse, G.; Furthmüller, J. *Comput. Mater. Sci.* **1996**, *6*, 15. (c) Kresse, G.; Furthmüller, J. *Phys. Rev. B: Condens. Matter Mater. Phys.* **1996**, *54*, 11169.

(20) Perdew, J. P.; Burke, S.; Ernzerhof, M. *Phys. Rev. Lett.* **1996**, *77*, 3865.

(21) Dudarev, S. L.; Botton, G. A.; Savrasov, S. Y.; Humphreys, C. J.; Sutton, A. P. *Phys. Rev. B: Condens. Matter Mater. Phys.* **1998**, *57*, 1505.

(22) (a) Dai, D.; Whangbo, M.-H. *J. Chem. Phys.* **2001**, *114*, 2887. (b) Dai, D.; Whangbo, M.-H. *J. Chem. Phys.* **2003**, *118*, 29.

Table 3. Relative Energies (in meV) of Seven Ordered Spin States of $Bi_4Cu_3V_2O_{14}$ Obtained from GGA+U Calculations

State	$U = 5$ eV	$U = 6$ eV	$U = 7$ eV
E_{AF1}	8.7	7.8	6.7
E_{AF2}	0	0	0
E_{AF3}	13.8	11.8	10
E_{AF4}	7.7	6.4	5.3
E_{AF5}	17.9	15.5	13.2
E_{AF6}	15.3	13.2	11.3
E_{AF7}	16.1	14.0	12

Table 4. Values of Spin Exchange Parameters (in meV) and Curie−Weiss Temperature (in K) of $Bi_4Cu_3V_2O_{14}$ Determined from GGA+U Calculations

	$U = 5$ eV	$U = 6$ eV	$U = 7$ eV
J_1	−1.9	−1.3	−0.9
J_2	−15.7	−13.1	−10.9
J_3	0.9	0.8	0.7
J_4	−18.7	−16.5	−14.3
J_5	−3.6	−2.9	−2.4
θ_{cal}	−212	−179	−151

interaction J_3 is weakly ferromagnetic. As depicted in Figure 4b, the spin−lattice given by J_2 and J_4 leads to an AFM interaction for the spin exchange path J_5, which reinforces the tendency for the AF2 spin arrangement because J_5 is antiferromagnetic. As already mentioned, this spin−lattice predicts an AFM spin ground state.

To determine how reasonable the calculated spin exchange parameters J_1−J_5 are, we calculated the Curie−Weiss temperature θ in terms of these parameters. In the mean field theory,[23] which is valid in the paramagnetic limit, θ is related to the spin exchange parameters of $Bi_4Cu_3V_2O_{14}$ as follows:

$$\theta = \frac{S(S+1)}{3k_B}\sum_i z_i J_i \qquad (15)$$

where the summation runs over all nearest neighbors of a given spin site, z_i is the number of nearest neighbors connected by the spin exchange parameter J_i, and S is the spin quantum number of each spin site (i.e., $S = 1/2$ in the present case). Thus, by employing the midpoint spin site of each linear spin timer unit, θ can be approximated by

$$\theta \approx \frac{2J_1 + 2J_2 + 2J_4}{4k_B} \qquad (16)$$

The θ values estimated by using the calculated spin exchange parameters (i.e., θ_{cal}) are summarized in Table 4. In magnitude, the θ_{cal} values are greater than the experimental value (i.e., −48.1 K) by a factor of approximately 3−4. This overestimation is not surprising because DFT electronic structure calculations generally overestimate the magnitude of spin exchange interactions by a factor of approximately up to 4.[22a,24,25]

4. Concluding Remarks

Both the spin dimer analysis based on EHTB calculations and the mapping analysis based on first principles DFT calculations show that the spin−lattice of $Bi_4Cu_3V_2O_{14}$ is not an AFM diamond chain but an AFM chain of linear AFM trimers that is made up of the SE interaction J_2 coupled through their midpoints through the SSE interaction J_4. Consequently, it is predicted that $Bi_4Cu_3V_2O_{14}$ has an AFM spin ground state and has no geometric spin frustration, both in agreement with experimental results. The AFM diamond model used for $Bi_4Cu_3V_2O_{14}$ arose from an idealized view of the structure of the Cu_4O_8 triple chain and the neglect of SSE interactions between neighboring Cu^{2+} ions. As has been pointed out,[11,12] small differences in the structural parameters associated with SE and SSE interactions can have profound effects on the strengths of their interactions, and SSE interactions can be much stronger than SE interactions. In interpreting the magnetic properties of a magnetic solid, the use of a spin−lattice deduced from the idealized geometrical arrangement of spin sites can be erroneous, and hence it is crucial to employ a spin−lattice determined from proper electronic structure calculations.

Acknowledgment. The work at Kyung Hee University was supported by Korean Research Foundation Grant KRF-2007-C00028 funded by the Korean Government (MOE-HRD, Basic Research Promotion Fund) and the work at North Carolina State University by the Office of Basic Energy Sciences, Division of Materials Sciences, U.S. Department of Energy, under Grant DE-FG02-86ER45259.

Supporting Information Available: Table S1 of the atomic orbital parameters employed in the present EHTB calculations. This material is available free of charge via the Internet at http://pubs.acs.org.

IC800216J

(23) Smart, J. S. *Effective Field Theory of Magnetism*; Saunders: Philadelphia, 1966.

(24) (a) Dai., D.; Koo, H.-J.; Whangbo, M.-H. *J. Solid State Chem.* **2003**, *175*, 341. (b) Dai, D.; Whangbo, M.-H.; Koo, H.-J.; Rocquefelte, X.; Jobic, S.; Villesuzanne, A. *Inorg. Chem.* **2005**, *44*, 2407.

(25) Grau-Crespo, R.; de Leeuw, N. H.; Catlow, C. R. *J. Mater. Chem.* **2003**, *13*, 2848.